Experimental Verification of Active Damping of Powertrain Vibrations with Simple Fuzzy Logic Compensation for Time-Varying Control Period

Heisei Yonezawa[#1]*, Ansei Yonezawa [#2], Takashi Hatano[#3],
Shigeki Hiramatsu[#3], Chiaki Nishidome [#4], Itsuro Kajiwara [#1]

#1
Division of Mechanical and Aerospace Engineering, Hokkaido University
N13, W8, Kita-ku, Sapporo 060-8628, Japan

#2
Division of Human Mechanical Systems and Design, Hokkaido University
N13, W8, Kita-ku, Sapporo 060-8628, Japan

#3
Mazda Motor Corporation
3-1 Shinchi, Fuchu-cho, Aki-gun, Hiroshima 730-8670, Japan

#4
CATEC Inc.
Ono-building 3F, 4-24-7, Taito, Taito-ku, Tokyo, 110-0016, Japan

* Corresponding author: yonezawah@eng.hokudai.ac.jp

Abstract

To ensure comfortability and lifetime of components, transient vibrations in a vehicle powertrain must be suppressed. This study proposes a novel active vibration control strategy with straightforward fuzzy inference compensation for time-fluctuations of control periods of engines used as actuators. First, a model prediction algorithm including a sampled-data controller (SDC) is applied for addressing the maximal phase lag of the control input caused by the fluctuated control period. Fluctuated renewal timings of the control input that are deviated from those of the periodical operated SDC are defined by fuzzy sets. These fuzzy sets are expressed as “Nearly past timing” and “Nearly future timing”. Using a human-intuition-like fuzzy compensation with only four inference rules, unknown control inputs at fluctuated update timings are reasonably determined from such fuzzy sets and periodical control signals given by the SDC. Experiments using an actual test device are performed to investigate the damping performance of the proposed control scheme. The experimental tests demonstrate that the novel active damping strategy significantly reduces transient vibrations despite the fluctuated control period. Moreover, several different test conditions newly reveal the robustness of the fuzzy compensation against fluctuations of variable regions in the control periods.

Keywords: Vibration control, Automotive drivetrain, Control period constraint, Sampled-data control, Fuzzy inference, Experimental verification

1. Introduction

Vehicles are susceptible to transient oscillations in a drivetrain due to abrupt changes in torque or gear backlash. Because such oscillations adversely impact a drivability, passenger comfort, and vehicle lifetime, many studies have investigated transient vibration control of powertrains. Examples include the model reference adaptive Linear Quadratic Tracking (ALQT) control,[1] linear-quadratic regulator (LQR) switching control,[2] and sliding mode control.[3,4] Especially, many controllers are based on model predictive control (MPC).[5–8] However, traditional MPC involves heavy optimization calculations and detailed modeling for complicated powertrain systems due to nonlinearities and mechanical constraints.

Active vibration control requires an actuator. Engines, which are a power source for powertrains, have been used as popular actuators for active damping because of their low cost and high power. Expectations for new engines based on clean energy such as hydrogen and biomass fuels have increased recently as well as implementations on existing HVs (Hybrid vehicles) and PHVs (Plug-in hybrid vehicles).[9] Consequently, an active vibration control using an engine[10] is an important topic.

However, the control period limits of engines engender a more challenging situation for active damping of powertrains. For example, the engine torque i.e., control input cannot be updated at regular intervals (Fig. 1). Updates can only occur once the crankshaft rotates to a predetermined angle. This restriction causes the following issues, which are main topics to be addressed in this study. First, the updating periods are much longer compared to the target resonant frequency to be suppressed, which adversely impacts the discretization errors when employing digital vibration control (issue (a)). Second, the control period of the actuator fluctuates over time because vehicle speed influences the update timing (issue (b)).

Previous studies have focused on engines that were used to evaluate the dynamics and control of powertrains, including HV-powered engines.[10–14] Real-time predictive controllers are promising approaches to address the engine delay.[10,11] The combination with another active damping actuator, i.e., a friction brake, can compensate for the slow dynamics of engines.[12] One study employed an adaptive disturbance observer-based harmonic rejection approach to handle the time-fluctuation dynamics.[13]

However, the above traditional methods did not simultaneously consider the issues (a) and (b). In addition, few works have focused on simplicity of the control systems, and an intuitive approach with the compensation mechanism to be easily handled has yet to be developed. Although the MPC-based approaches are promising, difficult tasks of accurately modeling for convoluted powertrain characteristics due to the control period constraint become barriers against providing simplicity for the control strategy.

Previously, we proposed an active vibration control system that partially considers the problem (b) in addition to the problem (a) caused by the control period constraint.[15] This approach is the MPC compensation based on a sampled-data H_2 controller to address the discrete error issue as well as the phase lag of the control input due to fluctuations in the control period. However, because our traditional approach handled just the maximum phase lag of control inputs, it did not consider fluctuations in the update timing. That is, problem (b) remains an issue.[15]

Fuzzy logic can quantitatively deal with ambiguities such as linguistic meanings. This powerful method expresses complex systems using membership functions and if-then logical inference rules. One of the superiorities is the robustness when the system cannot be accurately modeled. Although it has been applied to dynamics and vibration controls,[16,17] fuzzy logic has yet to be applied for vibration control of powertrains with time fluctuations.

In this paper, we propose a novel active vibration control strategy for a vehicle's drivetrain considering time-varying control input update timings. To handle inputs that cannot be updated at regular intervals, a sampled-data H_2 controller is combined with fuzzy logic. The former addresses the discretized error issue (problem (a)),[15] while the latter handles fluctuations in the update timing (problem (b)). The key concept of this strategy is that fuzzy logic is used when the update timing of the input diverges from that for the fixed periodic controller. The update timings are described using fuzzy sets: "Nearly previous timing," "Nearly upcoming timing," and "Nearly intermediate timing." Then using control commands computed by the fixed periodic controller, the above fuzzy sets, and human-intuition-like fuzzy rules, control inputs are determined at unpredicted (fluctuated) times. This fuzzy compensation is straightforward because it is composed only of four inference rules based on Tsukamoto-type fuzzy inference.

The three main contributions of this paper are described as follows. First, this study explicitly addresses various timings at which the actuator updates the control input (issue (b)). The proposed fuzzy logic compensation is based on the intuitive strategy imitating human-thinking-like qualitative decisions. Because it has only a few inference rules, the compensation mechanism is more simply realized. Detailed and complicated modeling of the variation of control input update timings is unnecessary in the proposed approach. This simpler fuzzy strategy is our originality compared with the above previous works. Second, a sampled data controller (hereafter, called as SDC) handles discretization errors (issue (a)) when using a digital controller over a long period. Thirdly, compared to the previous study that presents only simulation results and lacks critical experimental tests,[18] this paper performs experimental verifications under various test conditions using an actual test device to validate the proposed approach. This study employs a basic experimental device that was developed by simplifying a real vehicle drivetrain. The robustness of the proposed fuzzy system against fluctuations of the control periods is experimentally revealed.

2. Experimental system

2.1. Experimental device

A basic experimental device is used as the controlled object, whose specifications are shown in Table 1. To focus on the essence of vibration phenomena caused by abrupt changes in the driving force and backlash effects,[19–21] a diminished (i.e., simplified) structure is used to emulate a real drivetrain (Fig. 2). The structure represents a three-degrees-of-freedom oscillation model with mass points (M_E, m_G, M_B). A space is generated between the leaf springs on both sides of m_G to create a dead-zone band, which expresses backlash. The experimental device is more specifically described elsewhere.[19–21] The motor, which is combined with the control period constraint explained later, acts as the actuator.

Table 1 Specifications of the experimental device

Parameter	Value	Unit
M_B	0.232	kg
m_G	0.039	kg
M_E	1.04	kg
K_C	660.0	N/m
K_D	1.5×10^4	N/m
K_G	2.7×10^4	N/m
C_C	0.3	Ns/m
C_D	7.5	Ns/m
C_G	29.0	Ns/m
C_{cl}	4.0	Ns/m

2.2. Model

The experimental device contains nonlinearities including backlash. However, base vibration controller deign requires a linearized model. The plant's time varying linear state equation[15,19,20] is given as

$$\dot{\boldsymbol{x}}_p = \boldsymbol{A}_p \boldsymbol{x}_p + \boldsymbol{B}_{p1} \boldsymbol{w}_p + \boldsymbol{B}_{p2} u \tag{1}$$

$$y_p = \boldsymbol{C}_p \boldsymbol{x}_p + \boldsymbol{D}_{p1} \boldsymbol{w}_p + D_{p2} u \tag{2}$$

$$\boldsymbol{A}_p = \begin{bmatrix} 0 & 0 & 0 & 1 & 0 & 0 \\ 0 & 0 & 0 & 0 & 1 & 0 \\ 0 & 0 & 0 & 0 & 0 & 1 \\ -\frac{(K_D + K_C)}{M_B} & \frac{K_D}{M_B} & 0 & -\frac{(C_D + C_C)}{M_B} & \frac{C_D}{M_B} & 0 \\ \frac{K_D}{m_G} & -\frac{(SwK_G + K_D)}{m_G} & \frac{SwK_G}{m_G} & \frac{C_D}{m_G} & -\frac{(SwC_G + C_D)}{m_G} & \frac{SwC_G}{m_G} \\ 0 & \frac{SwK_G}{M_E} & -\frac{SwK_G}{M_E} & 0 & \frac{SwC_G}{M_E} & -\frac{(SwC_G + C_{cl})}{M_E} \end{bmatrix} \quad (3)$$

$$\boldsymbol{B}_{p1} = \begin{bmatrix} 0 & 0 & 0 & 0 & \frac{1}{m_G} & -\frac{1}{M_E} \\ 0 & 0 & 0 & \frac{1}{M_B} & 0 & 0 \end{bmatrix}^T, \quad \boldsymbol{B}_{p2} = \begin{bmatrix} 0 & 0 & 0 & 0 & 0 & \frac{1}{M_E} \end{bmatrix}^T$$

$$\boldsymbol{C}_p = [\,1 \quad 0 \quad 0 \quad 0 \quad 0 \quad 0\,], \ \boldsymbol{D}_{p1} = 0, \ \ D_{p2} = 0$$

$$\boldsymbol{x}_p = [X_B \quad x_G \quad X_E \quad \dot{X}_B \quad \dot{x}_G \quad \dot{X}_E]^T \quad (4)$$

where u denotes the control input and $\boldsymbol{w}_p$ shows the disturbance, which includes the backlash effect. Switching the parameter Sw represents the dead-zone characteristic of backlash. This is given as[22,23]

$$F = Sw \cdot K_G \cdot (X_E - x_G) + OKG$$

$$Sw = \begin{cases} 1, & X_E - x_G > |\delta| \\ 1, & X_E - x_G < -|\delta| \\ 0, & |X_E - x_G| \le |\delta| \end{cases}, \quad OKG = \begin{cases} -\big|K_G \times |\delta|\big|, & X_E - x_G > |\delta| \\ \big|K_G \times |\delta|\big|, & X_E - x_G < -|\delta| \\ 0, & |X_E - x_G| \le |\delta| \end{cases} \quad (5)$$

where $|\delta|$ and F indicate the dead zone width and the force by the rigidity K_G, respectively. In the SDC design, Sw = 1.0.

3. Long actuator control period with time fluctuations

3.1. Control period constraint

Figure 2(b) depicts the experimental device where a motor serves as the actuator. To investigate the issues (a) and (b) on the control period, only the essential part with respect to limitation of the control period that is equivalent to that of engines should be extracted. This is provided for the motor by a software of a digital signal processor (DSP). The control period constraint composed of the issues (a) and (b) is set via software in the experimental system. The conceptual closed-loop experimental configuration is demonstrated in Fig. 3(a). Although vibration control of DSP can compute control command signals at short and fixed periods, the update timings for the control inputs are restricted by long time-fluctuated control periods set via the latter program.

Among many different kinds of errors induced by the actual engine mechanism, this study focuses on the fluctuations in the update timing of the control input by the engine as an actuator, i.e., the errors of control periods due to time-fluctuations. That is, the errors that can be explicitly allowed by the proposed compensation are those of the time-fluctuated control period.

Figure 3(b) shows the fluctuation in the control period. Like those in Fig. 3(b), the experiments evaluated three fluctuation patterns. Limited by these fluctuated control periods, DSP holds the actual control input applied to the motor to the same value. From 2.0 to 4.0 s of Experiment 1 in Fig. 3(b), the updating frequency of the control input fluctuates from about 5.0 to 9.0 times the low resonant frequency (4 Hz) that is the target to be damped.

3.2. Fluctuations in the update timings

Figure 4 shows a conceptual diagram of the control command from a controller (black solid line) and the actual input generated (updated) by the actuator (red broken line). The main problem in this paper is clearly seen in Fig. 4.

The update timings of the actuator and that of the fixed periodic controller (operation period: ΔT_{cont}) diverge because the control period fluctuates. This phenomenon causes the control input's phase lag, which deteriorates the vibration control performance.

This study aims to determine the appropriate control commands to the actuator in time zone (T3) $k\Delta T_{cont} < t < (k+1)\Delta T_{cont}$ when the periodical control command values $u(k)$ at (T1) $t = k\Delta T_{cont}$ and $u(k+1)$ at (T2) $t = (k+1)\Delta T_{cont}$ are known.

4. Proposed active damping strategy

As shown in Fig. 5, the proposed strategy has two components: a model predictive algorithm including SDC[15] and straightforward fuzzy logic compensation for the fluctuations in update timings of the control inputs.

4.1. Model prediction algorithm using SDC

Employing digital controllers makes discretization errors more prominent because the update intervals of the input are forced to be increased. The previous studies[15,20] found that the control performance of a digital vibration controller deteriorates when the actuator control period is long. However, this issue can be avoided by using a sampled data controller (SDC).[24,25] This is due to its design and implementation process without any discretization. Here, a fixed periodic sampled data H_2 controller[24,25] is designed with a calculation period ΔT_{cont} because it is straightforward and easy to implement.

The control system design requires rough information on the controlled frequency band in which the resonance frequency can change. In this study, it is assumed that the resonance frequency 4 Hz in vehicle is known and included within the controlled frequency band. Because the SDC has the robustness, the proposed approach is considered to be applicable to small changes of the resonance frequency near 4 Hz within the control frequency band. In a generalized plant used to design SDC, the robustness is provided by frequency weighting functions, which are adjusted in such a way as to ensure the robustness.[15]

The sampled data H_2 controller is derived as a digital controller directly from the continuous-time plant shown in (1)–(4). Hence, discrete approximations are unnecessary in the implementation. The controller design is detailed elsewhere.[15] The resultant controller becomes a state equation in discrete-time domain, which is given as

$$\boldsymbol{x}_c(k+1) = \boldsymbol{A}_c\boldsymbol{x}_c(k) + \boldsymbol{B}_c\big(X_B(k\Delta T_{cont}) - r(k\Delta T_{cont})\big) \tag{6}$$

$$u(k) = \boldsymbol{C}_c\boldsymbol{x}_c(k) + D_c\big(X_B(k\Delta T_{cont}) - r(k\Delta T_{cont})\big) \tag{7}$$

$r(k\Delta T_{cont})$ represents the target signal, which is a step reference without vibrations under an abrupt driving force change of a real vehicle. $\boldsymbol{x}_c(k)$ is the state vector of the SDC. k represents the number of steps with respect to ΔT_{cont} (i.e., the calculation steps of the fixed periodic SDC). The measured output is the vehicle body vibration $y_p = X_B$. Combining (6), (7), and the feedforward input of the reference signal,[19,20] the control command $u(k)$ is computed at step $t = k\Delta T_{cont}$.

Second, as demonstrated in Fig. 4, the time fluctuating control period induces phase delays of the control input driving the actuator, deteriorating vehicle body vibrations. Here, the maximal phase lag $\varDelta T_{cont}$ alone is considered. To adequately compensate for ΔT_{cont}, the upcoming (future) command signal $u(k+1)$ from the SDC at $t=(k+1)\Delta T_{cont}$ must be obtained at step $t=k\Delta T_{cont}$. Herein a model predictive process with the time-varying linear Kalman filter is employed.[15] At step $t=k\Delta T_{cont}$ (Fig. 5), the iterative prediction with a minute cycle $\Delta T_{predict}$ provides $u(k+1)$ of upcoming (future) step $t=(k+1)\Delta T_{cont}$. The plant is online simulated from (T1) $t=k\Delta T_{cont}$ to (T2) $t=(k+1)\Delta T_{cont}$ with N_{pre} steps as

$$\begin{aligned}\boldsymbol{x}_{pd}[i+1] &= \boldsymbol{A}_{pd}\boldsymbol{x}_{pd}[i]+\boldsymbol{B}_{p1d}\boldsymbol{w}_p[i]+\boldsymbol{B}_{p2d}u[i]\\ &=\{\boldsymbol{I}_{\boldsymbol{6}\times\boldsymbol{6}}+\varDelta T_{predict}\cdot\boldsymbol{A}_p(t)\}\boldsymbol{x}_{pd}[i]+\{\varDelta T_{predict}\cdot\boldsymbol{B}_{p1}(t)\}\boldsymbol{w}_p[i]\\ &\quad+\{\varDelta T_{predict}\cdot\boldsymbol{B}_{p2}(t)\}u[i]\end{aligned} \tag{8}$$

$$y_{pd}[i]=\boldsymbol{C}_{pd}\boldsymbol{x}_{pd}[i]+\boldsymbol{D}_{p1d}\boldsymbol{w}_p[i]+D_{p2d}u[i]=\boldsymbol{C}_p(t)\boldsymbol{x}_{pd}[i] \tag{9}$$

where $i=1,\ 2,\ \cdots\ N_{pre}$ and $N_{pre}=(\varDelta T_{cont}/\varDelta T_{predict})+1$. Discrete-time systems (8) and (9) are derived online on the basis of the time-dependent-switched linear state equation of the experimental device containing nonlinearities such as backlash.[19,20] $u[i]$

represents the control input to drive the actuator, and $\boldsymbol{w}_p[i]$ indicates the external input, which includes the term on backlash.

The simulation requires initial conditions. Kalman filtering theory and the time-dependent-switched linear state equation are used to identify the state variable $\boldsymbol{x}_{pd}[i]$.[15,21]

The state-space representation of the SDC ($\boldsymbol{A}_c$, $\boldsymbol{B}_c$, $\boldsymbol{C}_c$, $\boldsymbol{D}_c$) with the calculation period ΔT_{cont} outputs $u(k+1)$ at $t = (k+1)\Delta T_{cont}$. Consequently, $u(k+1)$ can be predicted at step $t = k\Delta T_{cont}$ using the SDC included in the online simulation.

The information on backlash length is required for design of the proposed control system. Because this backlash value is related to the Kalman filter and the time-dependent-switched linear state equation, its changes may affect accuracy of the model prediction algorithm. In this study, a change in the value of backlash is assumed to be minute (quite small), and then high control performance is ensured under this assumption.

4.2. Straightforward fuzzy inference compensation for fluctuations in the update timing of the control input

Here, a straightforward fuzzy inference compensation strategy is proposed to determine the control inputs updated at fluctuated timings between $t = k\Delta T_{cont}$ and $t = (k + 1)\Delta T_{cont}$ (i.e., $k\Delta T_{cont} < t < (k + 1)\Delta T_{cont}$). Figure 5 depicts the fuzzy strategy applied within time zone (T3).

If the update timing of the actuator exactly coincides with $t = k\Delta T_{cont}$ or $t = (k + 1)\Delta T_{cont}$, then it is correct (i.e., logical) to command $u(k)$ or $u(k + 1)$ as the control input, respectively. However, if the timing of the control input update fluctuates, it diverges from that of the periodic sampled-data H_2 controller within $k\Delta T_{cont} < t <$

$(k+1)\Delta T_{cont}$. Here, inferring those control inputs updated at uncertain timings from known knowledge (e.g., IF $t=(k+1)\Delta T_{cont}$ then $u(t)=u(k+1)$) is defined as follows.

The main concept of the proposed strategy is that fuzziness is used to represent fluctuations in the update timing of the control inputs. The fuzziness is combined with the fixed periodic calculation timings of the sampled-data controller: upcoming (i.e., future) step $t=(k+1)\Delta T_{cont}$ and previous (i.e., past) step $t=k\Delta T_{cont}$. Specifically, fuzzy sets: approximately previous step $t=k\Delta T_{cont}$, approximately intermediate step $t=(k+1/2)\Delta T_{cont}$, and approximately upcoming step $t=(k+1)\Delta T_{cont}$ are defined to address the update timing of the control input that diverges from that of the fixed periodic controller. Then the degree of proximity (closeness) to the three update timings within $k\Delta T_{cont}<t<(k+1)\Delta T_{cont}$ is evaluated for the fluctuated update timing. Additionally, fuzziness for the control commands $u(k)$ at the previous step and

$u(k+1)$ at the upcoming step computed in Section 4.1 is employed to incorporate qualitative and intuitive (i.e., human-thought-like) knowledge, which states that

An unknown control input updated at a timing near $t = k\Delta T_{cont}$ $(t = (k+1)\Delta T_{cont})$ should be similar to $u(k)$ $(u(k+1))$.

Through an in-depth analysis of the factor: how close the fluctuated update timing within time zone (T3) is to those fixed steps?, an appropriate control input is reasonably inferred based on fuzzy sets Approximately $u(k)$ and Approximately $u(k+1)$.

The fuzzy inference rules also consider the amount of the time rate of change in control output. This corresponds to the absolute value of vehicle body velocity vibration $\dot{y}_p = \dot{X}_B$ for the controlled object in (1) and (2). Specifically, the inference rules employ the following intuitive insight:

If the fluctuation of the control output is larger in the future, the impact of the phase delay of the control input will become more worse. Thus, the predicted control input provides a more appropriate phase-delay compensation.

Consequently, our fuzzy if-then inference rules can be constructed as

(Rule 1):

IF (t^* is approximately future (ΔT_{cont})) THEN ($u(t^*)$ is approximately $u(k+1)$) (10)

(Rule 2):

IF (t^* is approximately past (0)) THEN ($u(t^*)$ is approximately $u(k)$) (11)

(Rule 3):

IF (t^* is approximately intermediate ($\frac{1}{2}\Delta T_{cont}$)) and ($|\dot{y}_p|$ is Big) THEN ($u(t^*)$ is approximately $u(k+1)$) (12)

(Rule 4):

IF (t^* is approximately intermediate ($\frac{1}{2}\Delta T_{cont}$)) and ($|\dot{y}_p|$ is Small) THEN ($u(t^*)$ is approximately $u(k)$) (13)

where t^*, which is the input variable, is given as $t^* = t - k\Delta T_{cont}$ within $0 < t^* < \Delta T_{cont}$ with respect to time t ($k\Delta T_{cont} < t < (k+1)\Delta T_{cont}$). The output variable $u(t^*)$ is the control input at that time (t^*). Herein Tsukamoto-type fuzzy inference[26,27] is employed for Rules 1–4 due to its simplicity.

For the input variable t^*, the fuzzy sets "approximately future (ΔT_{cont})," "approximately past (0)," and "approximately intermediate ($\frac{1}{2}\Delta T_{cont}$)" are defined as triangular membership functions h^t_{future}, h^t_{past}, and h^t_{middle}, respectively. For the input variable $|\dot{y}_p|$, "Big" and "Small" correspond to h^{cy}_{Big} and h^{cy}_{Small}, respectively.

$$h^t_{future} = \frac{1}{\Delta T_{cont}} \cdot t^* \tag{14}$$

$$h^t_{past} = -\frac{1}{\Delta T_{cont}} \cdot t^* + 1 \tag{15}$$

$$h^t_{middle} = \frac{2}{\Delta T_{cont}}\left(-\left|t^* - \frac{1}{2}\Delta T_{cont}\right| + \frac{1}{2}\Delta T_{cont}\right) \tag{16}$$

$$h^{cy}_{Big} = \frac{1}{|\dot{y}_p|_{max}} \cdot |\dot{y}_p| \tag{17}$$

$$h^{cy}_{Small} = -\frac{1}{|\dot{y}_p|_{max}} \cdot |\dot{y}_p| + 1 \tag{18}$$

$|\dot{y}_p|_{max}$ indicates the maximal value in the range of $|\dot{y}_p|$. Values above $|\dot{y}_p|_{max}$ are mapped to a membership degree of 0 or 1. That is, $|\dot{y}_p|_{max}$ is the tuning parameter for h^{cy}_{Small} and h^{cy}_{Big}. Given the real-time situation, the degree of fulfillment w_i $(0 \leq w_i \leq 1,\ i = 1, 2, \ldots 4)$ for the inference rules (Rules 1–4) is calculated in the antecedent part as

$$w_1 = h^t_{future}(t^*) \tag{19}$$

$$w_2 = h^t_{past}(t^*) \tag{20}$$

$$w_3 = h^t_{middle}(t^*) \times h^{cy}_{Big}(|\dot{y}_p|) \tag{21}$$

$$w_4 = h^t_{middle}(t^*) \times h^{cy}_{Small}(|\dot{y}_p|) \tag{22}$$

Next, reflecting the degree of match $w_1, w_2 \ldots w_4$ on the consequential part determines the outputs from the fuzzy inference rules. The fuzzy sets for the output variable: approximately $u(k+1)$ and approximately $u(k)$ are defined as h^u_{future} and h^u_{past}, respectively. In Tsukamoto-type fuzzy inference[26,27] monotonic membership functions (right-angled triangular) are employed as

$$h^u_{future} = \begin{cases} \dfrac{1}{\Delta u}(u - u(k)) \quad if \quad u(k) < u(k+1) \\ -\dfrac{1}{\Delta u}\big(u - u(k+1)\big) + 1 \quad if \quad u(k+1) < u(k) \end{cases} \tag{23}$$

$$h^u_{past} = \begin{cases} -\dfrac{1}{\Delta u}(u - u(k)) + 1 \quad if \quad u(k) < u(k+1) \\ \dfrac{1}{\Delta u}(u - u(k+1)) \quad if \quad u(k+1) < u(k) \end{cases} \tag{24}$$

where $\Delta u = |u(k+1) - u(k)|$. According to Tsukamoto-type fuzzy reasoning, the inference result u_i $(i = 1, 2, \dots 4)$ in each rule can be calculated by substituting $w_1, w_2 \dots w_4$ for the inverse function of $h^u_{future}(u)$ or $h^u_{past}(u)$, which is expressed as

(Case 1): $u(k) < u(k+1)$

$$u_1 = {h^u_{future}}^{-1}(w_1) = u(k) + w_1 \Delta u \tag{25}$$
$$u_2 = {h^u_{past}}^{-1}(w_2) = u(k) - (w_2 - 1)\Delta u \tag{26}$$
$$u_3 = {h^u_{future}}^{-1}(w_3) = u(k) + w_3 \Delta u \tag{27}$$
$$u_4 = {h^u_{past}}^{-1}(w_4) = u(k) - (w_4 - 1)\Delta u \tag{28}$$

(Case 2): $u(k+1) < u(k)$

$$u_1 = {h^u_{future}}^{-1}(w_1) = u(k+1) - (w_1 - 1)\Delta u \tag{29}$$
$$u_2 = {h^u_{past}}^{-1}(w_2) = u(k+1) + w_2 \Delta u \tag{30}$$
$$u_3 = {h^u_{future}}^{-1}(w_3) = u(k+1) - (w_3 - 1)\Delta u \tag{31}$$
$$u_4 = {h^u_{past}}^{-1}(w_4) = u(k+1) + w_4 \Delta u \tag{32}$$

Finally, the inference result $u_{Fuzzy}(t)$ to incorporate the four rules comprehensively is given as

$$u_{Fuzzy}(t) = \frac{\sum_{i=1}^{4} w_i u_i}{\sum_{i=1}^{4} w_i} \tag{33}$$

$u_{Fuzzy}(t)$ represents the input command within time-zone (T3) in Fig. 5 from the active powertrain vibration damping strategy.

5. Experimental verification and discussion

The effectiveness of the active damping strategy is experimentally verified using the system shown in Figs. 2 and 3. The goal is to achieve an ideal step signal by the control objective, i.e., damping the vehicle vibration X_B. The major change in the ideal response that involves no vibrations goes from a negative value towards a positive one at 2.0 s. It is motivated from the situation with an abrupt driving force change in real vehicles. This situation can clearly evaluate the transient vibrations induced in the vehicle body.

The experiments compare the proposed transient vibration control strategy to the traditional SDC without compensation for the fluctuating update timing of the control input. ΔT_{cont} of the fixed periodic SDC and the predictive calculation interval $\Delta T_{predict}$ were set to be 0.0438 s and 0.8 ms, respectively. The verification condition with the control period $\Delta T_{cont} = 0.0438\,\mathrm{s}$ corresponds to a vehicle driving condition with suppressed speed of about 600-700rpm in a 4-cylinder engine.

The results of the experiments are shown in Figs. 6-8, which are based on the control period constraints like Experiments 1–3 indicated in Fig. 3(b), respectively. The upper graph depicts the time response waveforms of the vehicle vibrations, while the lower one shows that for the control inputs. The blue, green, and black lines denote the responses without any control, the ideal response, responses by using only the SDC without compensation, respectively. The red lines show the experimental results obtained by the proposed method.

Comparing the waveforms with only the SDC (black lines) and the proposed vibration control strategy (red lines) in Figs. 6–8 highlights the effectiveness of the proposed fuzzy logic compensation. Only use of the SDC (sampled data H_2 controller) barely dampens the vibrations due to the phase delays on the actual inputs, deteriorating the transient performance. In contrast, the proposed strategy exhibits excellent transient characteristics, indicating that the vibrations induced after 2.0 s are greatly reduced. The compensations for different update timings of the control input within $k\Delta T_{cont} < t < (k+1)\Delta T_{cont}$ lead to the improvement of the performances. Thus, the fuzzy logic can realize appropriate vibration control commands, even if the update timing fluctuates.

Figure 9 is a magnified view of the control input signals calculated in the vibration control system with the fuzzy inference and SDC in Experiment 1. In every step, the control command value of $u(k)$ (green waveform) follows the predicted input signal of $u(k+1)$ (magenta waveform). Hence, it is considered that the predictive algorithm well works. The agreement of the predicted values $u(k+1)$ with the one-step-later command values $u(k)$ demonstrates that the predictive process has a suitable accuracy. This tendency leads to the reasonable fuzzy logic commands.

The proposed strategy improves the transient response in all conditions of Figs. 6–8, even though Figs. 6-8 tested the totally different control period constraints (i.e., Experiments 1-3). Compared to the case of applying only SDC (black lines), the transient vibrations with the proposed method (red lines) are significantly suppressed. These results experimentally reveal the robustness of the proposed method and are produced despite fragmentary modeling of drivetrain dynamics that do not include a time-fluctuating control period. This fact implies that fuzzy logic is responsible for the robustness.

As shown in Figs. 6-8, the proposed approach can explicitly address variations of the control period. This is because the fuzzy compensation has the robustness against uncertainty in the update timing of the control input. However, the proposed approach assumes that the accuracy of the control input value (i.e., torque value generated from the actual engine) is sufficient. In other words, the variations (errors) of the control input accuracy with life, temperature and usage are not explicitly considered, and therefore they may affect vibration control performance. Hence, it will be necessary to investigate the robustness of the proposed approach against those effects in the future.

Table 2 quantitatively compares the damping performances of each result in Figs. 6-8.

The 2-norm of the error between the vehicle body oscillation and the ideal step signal is presented. In all of Figs. 6-8, the smallest value is realized by the proposed strategy, meaning the improvement of the vibration reductions by the fuzzy inference compensation. For example, compared to “W/o control” and “W/o compensation”, the 2-norm with the proposed strategy is decreased by 76.9036% and 75.6307% in Fig. 6.

For actual vehicles, the proposed approach focuses on only the use case under consideration of a tip-in coming from low to high torque. That is, the working condition assumed in this study has a backlash traversal only at beginning and the backlash angle is fixed afterwards. This is one of the limitations of the proposed approach for actual vehicle application. To realize the application to an actual vehicle, the proposed active damping strategy should be improved so as to also work well with the use case of a tip-out coming from high to low torque. This will be included in our future tasks. One of the promising plans is to combine the proposed method with an online adaptive mechanism so as to be flexibly applied to changes of the lash angle during vibration.

Table 2 Quantitative results of comparing the damping performances via 2-norm of each error between the vehicle body oscillation and the ideal step signal

Each experiment result	2-norm in Fig. 6	2-norm in Fig.7	2-norm in Fig. 8
W/o control	0.9555	0.9764	0.9407
W/o compensation	0.9056	0.7156	0.6044
Proposed strategy	0.2207	0.4218	0.4078

The proposed strategy has other limitations. First, the parameters were manually tuned. Second, the experiments were conducted only for the simplified drivetrain. In the future, inspired by the existing works[28,29], we plan to apply the fuzzy logic in conjunction with optimization algorithms to real test vehicles, aiming at resolving the above residual issues.

6. Conclusion

A straightforward fuzzy logic compensation was proposed for active vibration control of powertrains when the update timing of the control input fluctuates over time in the actuator. The proposed strategy combines a model prediction algorithm, the SDC, and the new fuzzy logic compensation. The main concept is that fuzzy sets are used to represent fluctuations in the update timing of the control inputs that diverges from that of the fixed periodic SDC. Using such fuzzy sets, periodic control commands given by the SDC, and a human-intuition-like fuzzy inference composed of only four rules, we can reasonably determine appropriate control inputs at fluctuated update timings. Experiments validated the effectiveness of the proposed strategy. The comparative tests verified that the strategy improves the damping performance as well as the robustness.

Declaration of competing interest

The authors declare that there is no conflict of interest.

Funding

The authors disclosed receipt of the following financial support for the research, authorship, and/or publication of this article: This work was partly supported by Japan Society for the Promotion of Science (JSPS) KAKENHI [Grant Number JP 20J11084].

References

1. Yue Y, Huang Y, Hao D, et al. Model reference adaptive LQT control for anti-jerk utilizing tire-road interaction characteristics. *Proc Inst Mech Eng Part D J Automob Eng* 2021; 235: 1670–1684.
2. Templin P, Egardt B. A Powertrain LQR-Torque Compensator with Backlash Handling. *Oil Gas Sci Technol – Rev d'IFP Energies Nouv* 2011; 66: 645–654.
3. Lv C, Zhang J, Li Y, et al. Mode-switching-based active control of a powertrain system with non-linear backlash and flexibility for an electric vehicle during regenerative deceleration. *Proc Inst Mech Eng Part D J Automob Eng* 2015; 229: 1429–1442.
4. Zhou Z, Guo R, Liu X. A disturbance-compensation-based sliding mode control scheme on mode switching condition for hybrid electric vehicles considering nonlinear backlash and stiffness. *J Vib Control* 2022; 107754632210961.
5. Lu X, Lu T, Chai B. Mode-switch model predictive controller with "pre-contact" method for alleviating driveline vibration of electric vehicles considering backlash. *Proc Inst Mech Eng Part D J Automob Eng* 2020; 234: 2176–2194.
6. Atabay O, Ötkür M, Ereke İM. Model based predictive engine torque control for improved drivability. *Proc Inst Mech Eng Part D J Automob Eng* 2018; 232: 1654–1666.
7. Chen X, Peng D, Hu J, et al. Adaptive torsional vibration active control for hybrid electric powertrains during start-up based on model prediction. *Proc Inst Mech Eng Part D J Automob Eng* 2021; 095440702110561.
8. Yüceşan A, Mugan A. Development of a model predictive controller for an active torsional vibration damper to suppress torsional vibrations in vehicle powertrains. *Proc Inst Mech Eng Part D J Automob Eng* 2022; 236: 127–141.
9. Sarwar MH, Shah MA, Islam SU, et al. Fuzzy Logic-Based Novel Hybrid Fuel Framework for Modern Vehicles. *IEEE Access* 2020; 8: 160596–160606.
10. Berriri M, Chevrel P, Lefebvre D. Active damping of automotive powertrain oscillations by a partial torque compensator. *Control Eng Pract* 2008; 16: 874–

883.
11. Baumann J, Torkzadeh DD, Ramstein A, et al. Model-based predictive anti-jerk control. *Control Eng Pract* 2006; 14: 259–266.
12. Mattsson M, Mehler R, Jonasson M, et al. Optimal Model Predictive Acceleration Controller for a Combustion Engine and Friction Brake Actuated Vehicle. *IFAC-PapersOnLine* 2016; 49: 511–518.
13. Vadamalu RS, Beidl C. Adaptive internal model-based harmonic control for active torsional vibration reduction. *IEEE Trans Ind Electron* 2020; 67: 3024–3032.
14. Huang Y, Wang J, Yue Y, et al. Model predictive control for active vibration suppression of hybrid electric vehicles during mode transition. *Proc Inst Mech Eng Part D J Automob Eng* 2022; 095440702211173.
15. Yonezawa H, Kajiwara I, Nishidome C, et al. Active vibration control of automobile drivetrain with backlash considering time-varying long control period. *Proc Inst Mech Eng Part D J Automob Eng* 2021; 235: 773–783.
16. Wang H, Lu Y, Tian Y, et al. Fuzzy sliding mode based active disturbance rejection control for active suspension system. *Proc Inst Mech Eng Part D J Automob Eng* 2020; 234: 449–457.
17. Li Z, Li J, Zhou Q, et al. Intelligent air/fuel ratio control strategy with a PI-like fuzzy knowledge–based controller for gasoline direct injection engines. *Proc Inst Mech Eng Part D J Automob Eng* 2019; 233: 2161–2173.
18. Yonezawa H, Yonezawa A, Hatano T, et al. Fuzzy-reasoning-based robust vibration controller for drivetrain mechanism with various control input updating timings. *Mech Mach Theory* 2022; 175: 104957.
19. Yonezawa H, Kajiwara I, Sato S, et al. Vibration control of automotive drive system with nonlinear gear backlash. *J Dyn Syst Meas Control Trans ASME* 2019; 141: 1–11.
20. Yonezawa H, Kajiwara I, Nishidome C, et al. Vibration control of automotive drive system with backlash considering control period constraint. *J Adv Mech Des Syst Manuf* 2019; 13: 1–16.
21. Yonezawa H, Kajiwara I, Sato S, et al. Application of physical function model to

state estimations of nonlinear mechanical systems. *IEEE Access* 2021; 9: 12002–12018.

22. Gerdes JC, Kumar V. An impact model of mechanical backlash for control system analysis. In: *Proceedings of 1995 American Control Conference - ACC'95*. American Autom Control Council, pp. 3311–3315.
23. Nordin M, Galic' J, Gutman P-O. New models for backlash and gear play. *Int J Adapt Control Signal Process* 1997; 11: 49–63.
24. Bamieh B, Boyd Pearson J. The H2 problem for sampled-data systems. *Syst Control Lett* 1992; 19: 1–12.
25. Khargonekar PP, Sivashankar N. H2 optimal control for sampled-data systems. *Syst Control Lett* 1991; 17: 425–436.
26. Gupta PK, Muhuri PK. Extended Tsukamoto's inference method for solving multi-objective linguistic optimization problems. *Fuzzy Sets Syst* 2019; 377: 102–124.
27. Suharjito, Diana, Yulyanto, et al. Mobile Expert System Using Fuzzy Tsukamoto for Diagnosing Cattle Disease. *Procedia Comput Sci* 2017; 116: 27–36.
28. Eckert JJ, Barbosa TP, Silva FL, et al. Optimum fuzzy logic controller applied to a hybrid hydraulic vehicle to minimize fuel consumption and emissions. *Expert Syst Appl* 2022; 207: 117903.
29. Eckert JJ, da Silva SF, Santiciolli FM, et al. Multi-speed gearbox design and shifting control optimization to minimize fuel consumption, exhaust emissions and drivetrain mechanical losses. *Mech Mach Theory* 2022; 169: 104644.

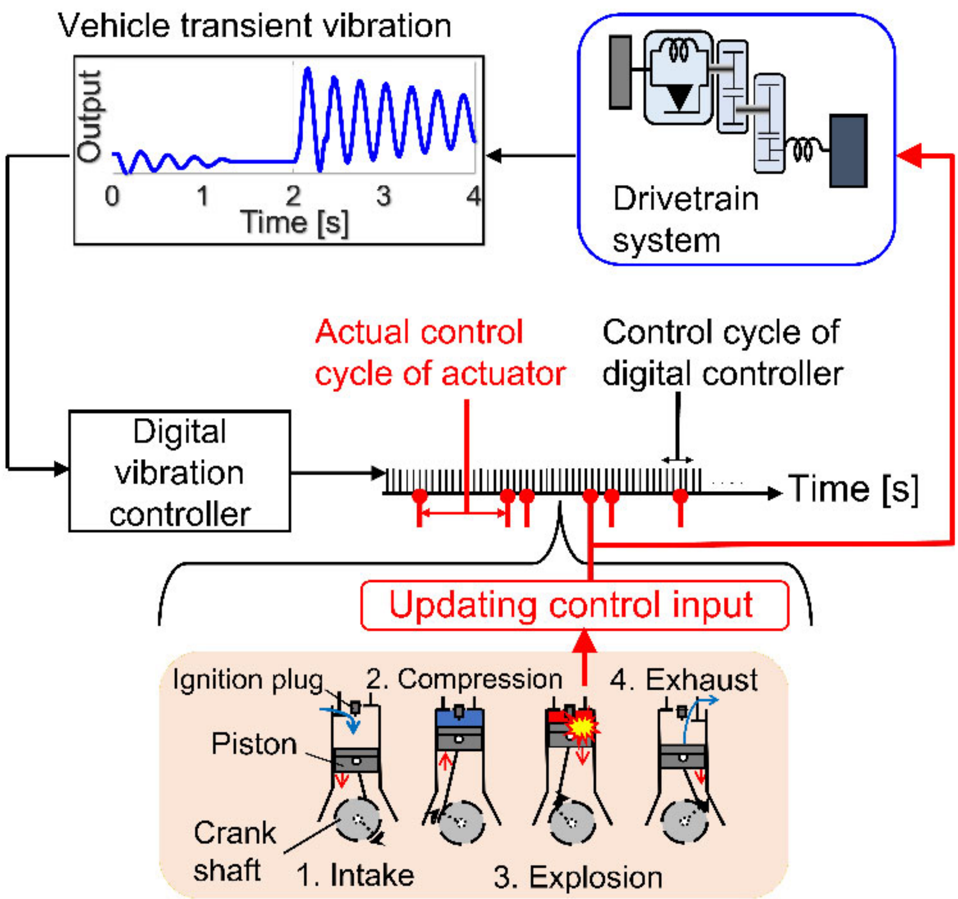

Figure 1. Limitation of the control period due to the mechanism generating engine torque.

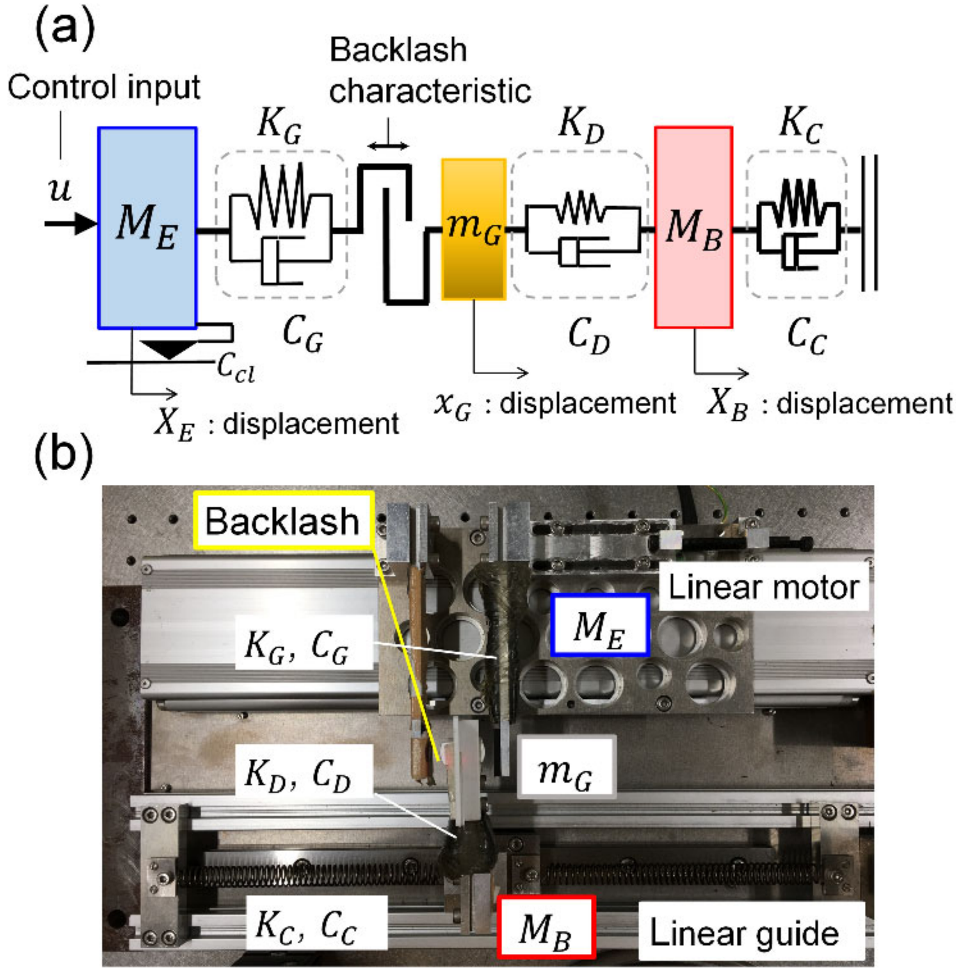

Figure 2. Experimental device of simplified drivetrain: (a) dynamical model and (b) real mechanism.

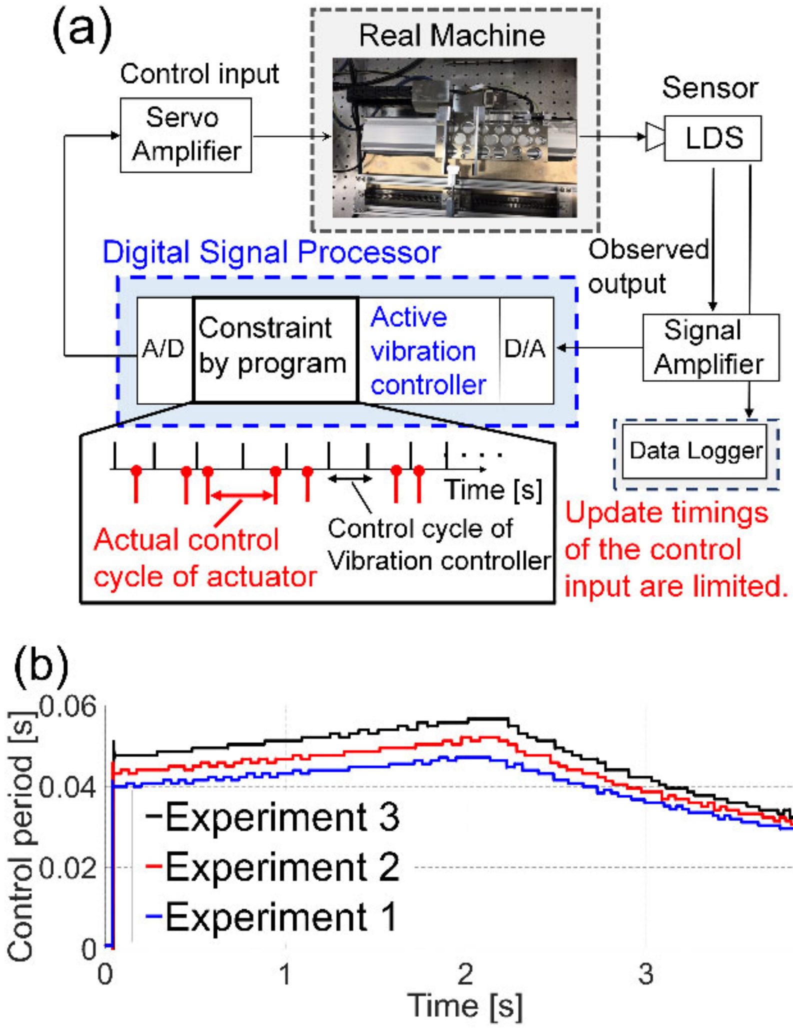

Figure 3. Experimental setup: (a) conceptual closed-loop system and (b) three patterns of control period constraints.

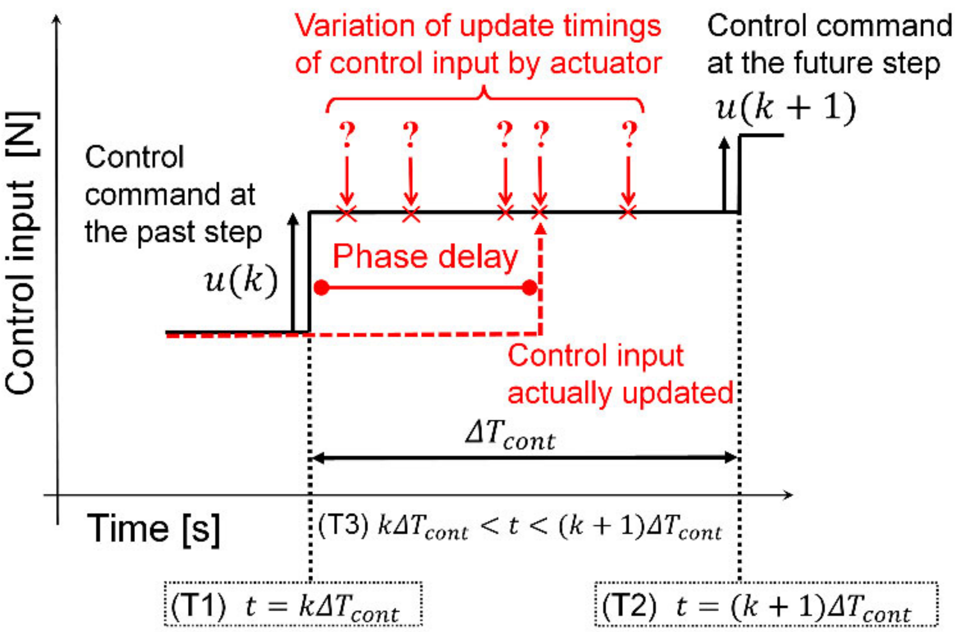

Figure 4. Variation of updating timings of actual control inputs from those of a fixed periodical damping controller.

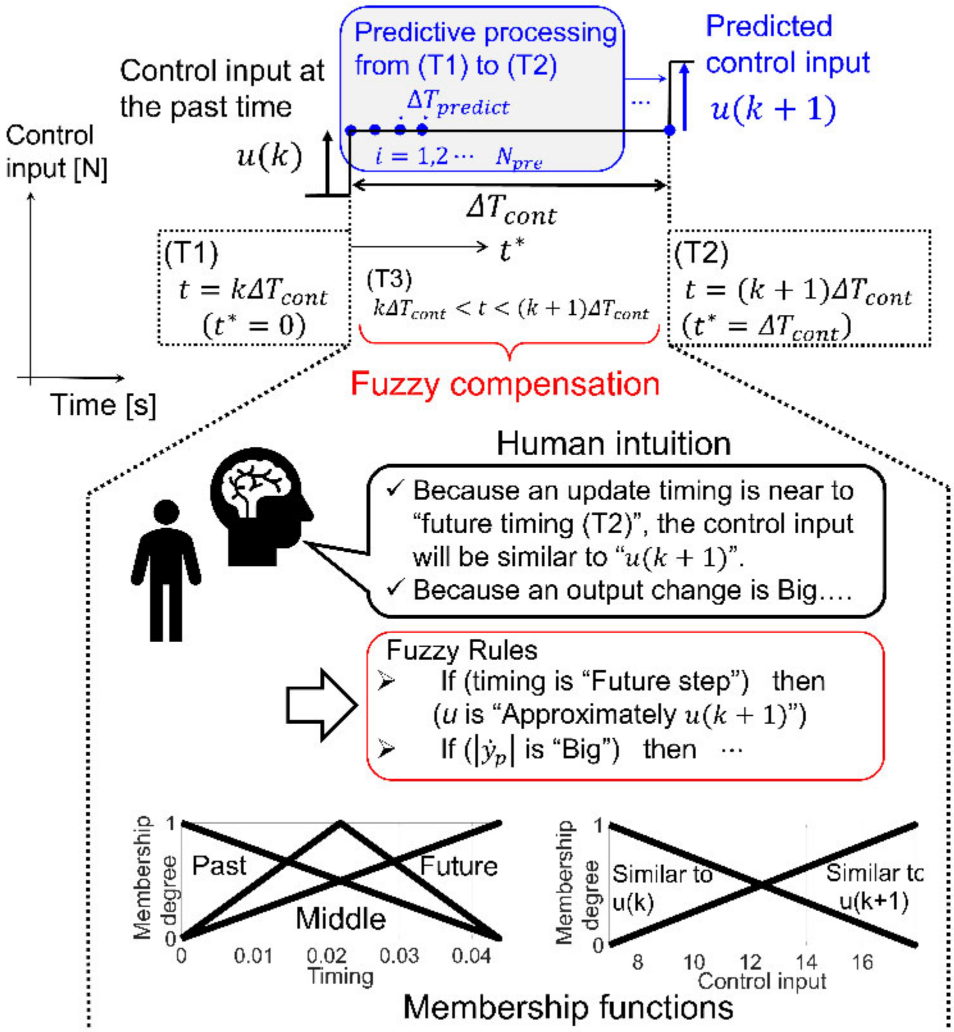

Figure 5. Outline of proposed entire control scheme.

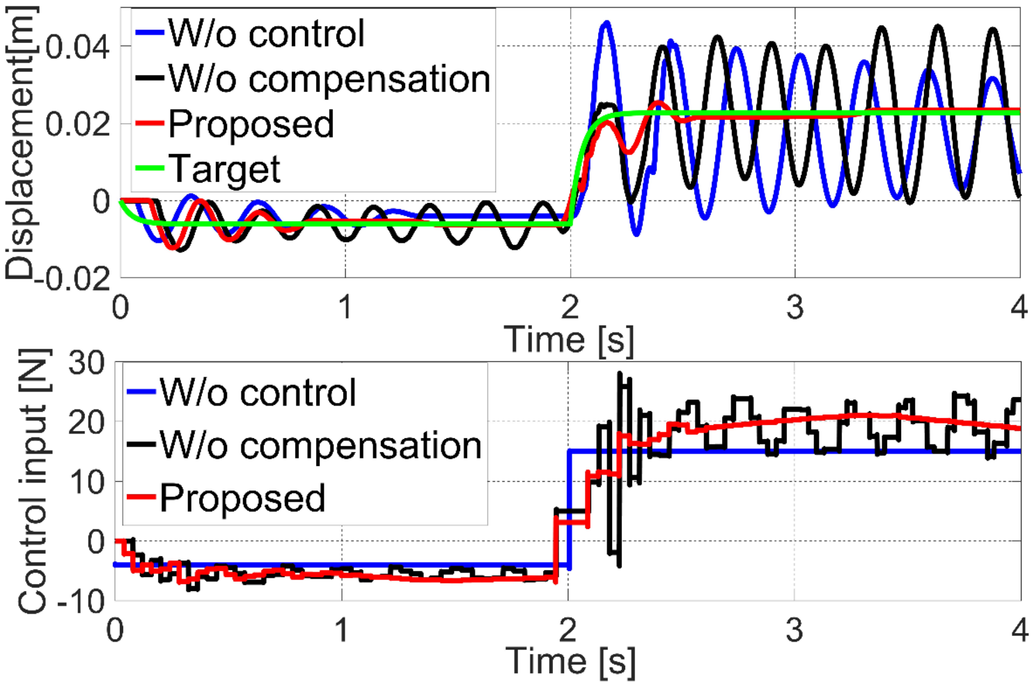

Figure 6. Vehicle body vibrations and control inputs obtained by the experiments (control period constraints: Experiment 1).

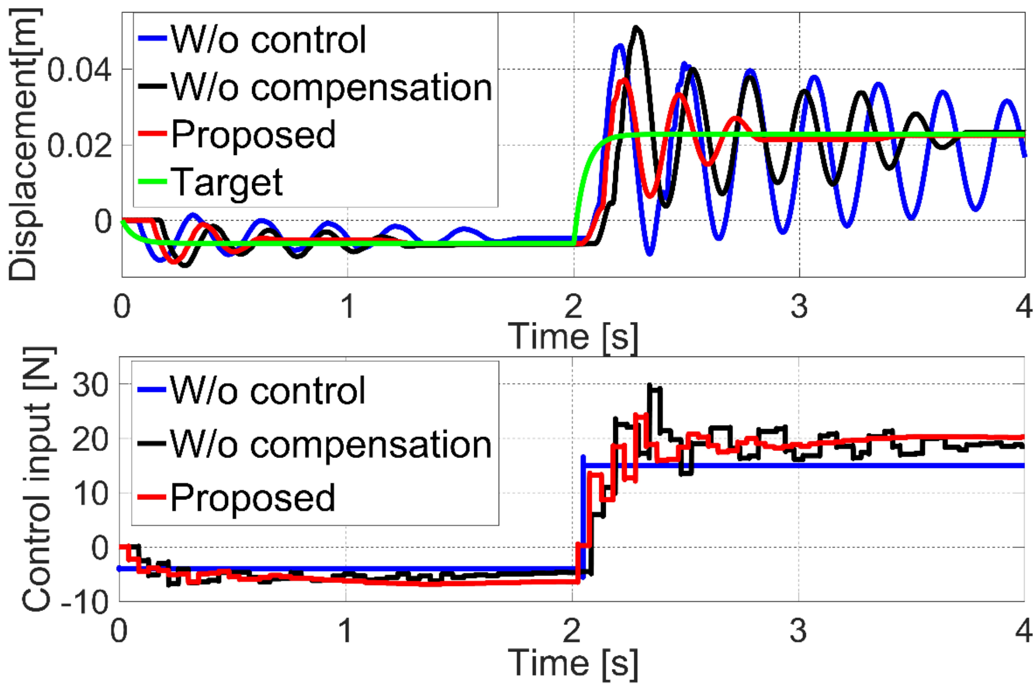

Figure 7. Vehicle body vibrations and control inputs obtained by the experiments (control period constraints: Experiment 2).

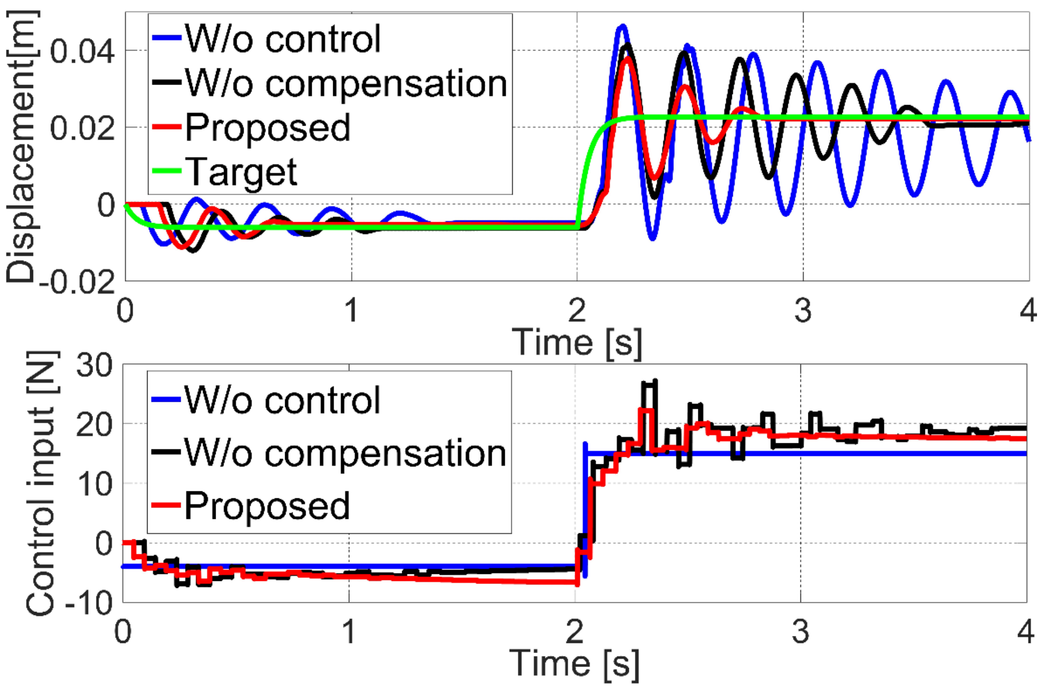

Figure 8. Vehicle body vibrations and control inputs obtained by the experiments (control period constraints: Experiment 3).

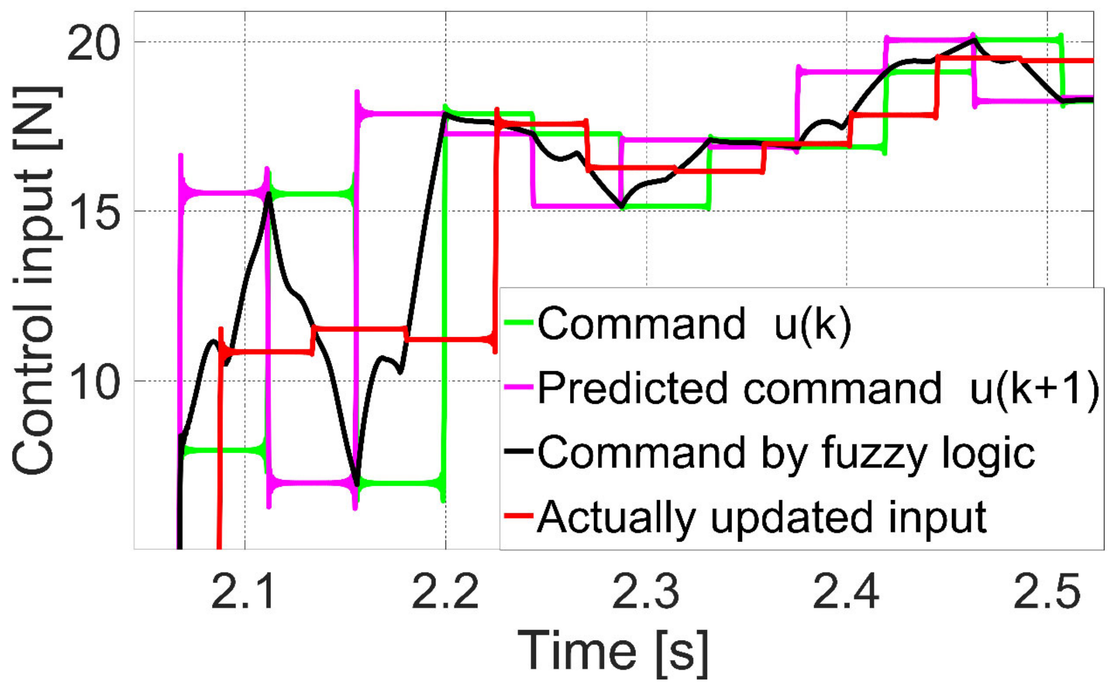

Figure 9. Enlarged plot of the control commands calculated by the proposed active damping strategy.